0022-3565/11/3363-973–982$20.00
THE JOURNAL OF PHARMACOLOGY AND EXPERIMENTAL THERAPEUTICS
JPET 336:973–982, 2011

Vol. 336, No. 3
172171/3671595
Printed in U.S.A.

Pregabalin Modulation of Neurotransmitter Release Is Mediated by Change in Intrinsic Activation/Inactivation Properties of $Ca_V2.1$ Calcium Channels[S]

Mariano N. Di Guilmi, Francisco J. Urbano, Carlota Gonzalez Inchauspe, and Osvaldo D. Uchitel

Instituto de Fisiología, Biología Molecular y Neurociencias, Consejo Nacional de Investigaciones Científicas y Técnicas, and Departamento de Fisiología, Biología Molecular y Celular, Facultad de Ciencias Exactas y Naturales, Universidad de Buenos Aires, Argentina

Received June 29, 2010; accepted December 21, 2010

ABSTRACT

In this work, we studied the effects of the anticonvulsant and analgesic drug pregabalin (PGB) on excitatory postsynaptic currents (EPSCs) at principal neurons of the mouse medial nucleus of the trapezoid body and on presynaptic calcium currents at the calyx of Held. We found that the acute application of PGB reduced the amplitude of EPSCs in a dose-dependent manner with a maximal blocking effect of approximately 30%. A clinical high-concentration dose of PGB (e.g., 500 μM) blocked $Ca_V2.1$ channel-mediated currents and decreased their facilitation during a 100-Hz train, without changing their voltage-dependent activation. Furthermore, PGB also removed the inactivation of $Ca_V2.1$ channels at a clinically relevant low concentration of 100 μM. These results suggest novel modulatory mechanisms mediated by the acute administration of PGB on fast excitatory synaptic transmission and might contribute to better understanding PGB anticonvulsant/analgesic clinical effects.

Introduction

Pregabalin (PGB) [*S*-(+)-3-isobutyl-GABA] is a blood-brain barrier-crossing drug with anticonvulsant and analgesic actions without any known effect on either $GABA_A$ or $GABA_B$ receptors (Taylor et al., 1998; Maneuf et al., 2003) . Although PGB is being used for the treatment of epilepsy and neuropathic pain, its mechanism of action is still not fully understood. The pharmacological actions of PGB (Belliotti et al., 2005; Taylor et al., 2007) are dependent on its high-affinity binding to the α_2-δ auxiliary subunit of voltage-gated calcium channels (Gee et al., 1996; Taylor and Garrido, 2008). This mechanism is especially interesting, considering that auxiliary subunits, such as α_2-δ, are known to modulate membrane trafficking of calcium channels as well as their kinetic properties (Qin et al., 1998; Klugbauer et al., 2003). In addition, an intracellular action of PGB, mediated by the L-amino acid transporter, has been suggested (Cunningham et al., 2004). Chronic PGB could play an active role in calcium channel trafficking (Hendrich et al., 2008). Using mutant subunits that do not bind gabapentin, Hendrich et al. (2008) showed that the effects on channel trafficking were via $\alpha_2\delta$-1 and $\alpha_2\delta$-2. Furthermore, gabapentin has been involved in cortical synaptic maturation in mice (Eroglu et al., 2009), in such a way that gabapentin receptor α_2-δ subunits were required during early developmental stages of cortical excitatory synaptic transmission.

On the other hand, it has been shown that acute application of either PGB or gabapentin reduced calcium currents

This work was supported by the Wellcome Trust [Grant 084636]; Agencia Nacional de Ciencia y Tecnología-Fondo para la Investigación Científica y Tecnológica [Grant 6220]; Proyectos de la Universidad de Buenos Aires para la Investigación Científico-Tecnológica [Grants UBACYT-X171, UBACYT-X223]; Agencia Nacional de Promoción Científica y Tecnológica-Fondo para la Investigación Científica y Tecnológica, Banco Interamericano de Desarrollo-Proyectos de Investigación Científica y Tecnológica [Grants PICT-2005-32,113, PICT-2005-13,367, PICT-2006-199] (to O.D.U.); Agencia Nacional de Promoción Científica y Tecnológica-Fondo para la Investigación Científica y Tecnológica, Banco Interamericano de Desarrollo-Proyectos de Investigación Científica y Tecnológica [Grants PICT-2007-1009, PICT-2008-2019]; and Agencia Nacional de Promoción Científica y Tecnológica-Proyectos de Investigación para la Radicación/Relocalización de Investigadores-Programa de Recursos Humanos [Grant PIDRI-PRH- 2007–1] (to O.D.U.).

Article, publication date, and citation information can be found at http://jpet.aspetjournals.org.

doi:10.1124/jpet.110.172171.

[S] The online version of this article (available at http://jpet.aspetjournals.org) contains supplemental material.

ABBREVIATIONS: PGB, pregabalin; MNTB, medial nucleus of the trapezoid body; IpCa, presynaptic calcium current(s); EPSC, excitatory postsynaptic current; aCSF, artificial cerebrospinal fluid; TEA-Cl, tetraethyl ammonium chloride; QX-314, *N*-(2,6-diethylphenylcarbamoylmethyl)-triethyl-ammonium chloride; TTX, tetrodotoxin; AP, action potential; PP, prepulse; TP, text pulse; ANOVA, analysis of variance; mEPSC, miniature excitatory postsynaptic current; IP, interpulse; BK, big conductance; SK, small conductance.

(for review, see Taylor et al., 2007), by interacting with α_2-δ auxiliary subunits (Stefani et al., 1998; Martin et al., 2002; Sutton et al., 2002). Concomitantly, PGB reduces evoked postsynaptic responses (Cunningham et al., 2004; Joshi and Taylor, 2006; Micheva et al., 2006). In contrast, studies with recombinant voltage-gated calcium channels have not shown any acute effect of PGB on channel function (Hendrich et al., 2008). Furthermore, electrophysiological recordings have failed to describe acute gabapentin-mediated changes in calcium channel currents recorded from Purkinje cells or from human hippocampal neurons. Despite the contradictory effects of PGB on calcium currents, most of the studies in which the effect of this compound on transmitter release was analyzed showed a reduced release of various neurotransmitters from synapses in several neuronal tissues (Taylor et al., 2007).

The aim of this work was to study the acute PGB mechanism of action on excitatory neurotransmitter release at the principal neurons of mouse medial nucleus of the trapezoid body (MNTB) (Schneggenburger and Forsythe, 2006). This in vitro model consists of an axosomatic glutamatergic synapse (calyx of Held) onto MNTB neurons, which functions as a relay in the binaural auditory brainstem computing sound source localization (Schneggenburger and Forsythe, 2006). Because of the large size of presynaptic terminals and their accessibility to a patch-clamp pipette, it is possible to directly measure both presynaptic calcium currents (I_{pCa}) from the calyx of Held and excitatory postsynaptic currents (EPSCs) from the soma of the MNTB neurons (Schneggenburger and Forsythe, 2006). PGB-mediated modulation of both presynaptic $Ca_v2.1$ (P/Q-type) calcium currents and EPSCs was studied.

We observed that PGB reduced the amplitude of EPSCs at the calyx of Held synapses with a dose-dependent blocking effect that reached a maximum plateau of ~30%. The amplitude of presynaptic $Ca_v2.1$ (P/Q-type) calcium currents decreased, although to a lesser extent, in the presence of PGB, whereas no differences were observed in their voltage activation properties. A larger rescue from inactivation of $Ca_v2.1$ presynaptic channels was induced by both 100 and 500 μM PGB (i.e., plasma concentrations expected during single and repetitive clinical administrations of PGB, respectively). Our results indicate that PGB significantly alters synaptic glutamatergic neurotransmission by modulation of presynaptic calcium channels.

Materials and Methods

Preparation of Brainstem Slices. Experiments were performed in accordance with the UK Animals (Scientific Procedures) Act 1986. Fifty 11- to 15-day-old mice were used in this study. Brain was removed rapidly after decapitation and placed into an ice-cold low-sodium artificial cerebrospinal fluid (aCSF). The brainstem was glued on a Peltier chamber of an Integraslice 7550PSDS vibrating microslicer (Campden Instruments Ltd., Leicester, UK). Transverse slices containing the MNTB were cut sequentially and transferred to an incubation chamber containing normal aCSF with low calcium/high magnesium (0.5 mM $CaCl_2$ and 3 mM $MgCl_2$) at 37°C for 1 h. Slices were then allowed to rest at room temperature. Slices of 200- and 300-μm thickness were used for presynaptic Ca^{2+} current and EPSC recording experiments, respectively. Normal aCSF contained 125 mM NaCl, 2.5 mM KCl, 26 mM $NaHCO_3$, 1.25 mM NaH_2PO_4, 10 mM glucose, 0.5 mM ascorbic acid, 3 mM myo-inositol, 2 mM sodium pyruvate, 1 mM $MgCl_2$, and 2 mM $CaCl_2$. Low sodium aCSF was obtained from normal aCSF, replacing NaCl by 250 mM sucrose and changing both $MgCl_2$ and $CaCl_2$ concentrations to 2.9 and 0.1 mM, respectively. The pH was 7.4 when gassed with 95% O_2-5% CO_2.

Whole-Cell Patch-Clamp Recordings. Slices were transferred to an experimental chamber continuously aerated with 95% O_2-5% CO_2 saturated normal aCSF at room temperature (22–25°C). MNTB neurons were visualized using Nomarski optics of an Eclipse E600-FN (Nikon, Tokyo, Japan) microscope, and a 60×, 1 numerical aperature water immersion objective lens (Nikon). Whole-cell voltage-clamp recordings were made with patch pipettes pulled from thin-walled borosilicate glass (GC150F-15; Harvard Apparatus, Kent, UK). Electrodes had resistances of 3.6 to 4.2 MΩ for presynaptic recordings and 3.0 to 3.5 MΩ for postsynaptic recordings, when filled with internal solution. Patch solutions for voltage-clamp recordings contained: 110 mM CsCl, 40 mM Hepes, 10 mM TEA-Cl, 12 mM Na_2-phosphocreatine, 1 mM EGTA, 2 mM MgATP, 0.5 mM LiGTP, and 1 mM $MgCl_2$. The pH was adjusted to 7.3 with CsOH. To block Na^+ currents and avoid postsynaptic action potentials, 10 mM *N*-(2,6-diethylphenylcarbamoylmethyl)-triethyl-ammonium chloride (QX-314) was added when EPSCs were recorded. Lucifer yellow (1–3 mg/ml) was also included to the pipette solution to visually confirm that presynaptic terminals were recorded.

Whole-cell patch-clamp recordings were made using an Axopatch 200B amplifier (Molecular Devices, Sunnyvale, CA), a Digidata 1200 digitizer (Molecular Devices), and pClamp 9.0 software (Molecular Devices). Electrophysiology data were sampled at 50 kHz and filtered at 4 to 6 kHz (low-pass Bessel filer). Series resistance values ranged from 6 to 15 MΩ, for both pre- and postsynaptic recordings and were compensated for by up to 60%. Whole-cell membrane capacitances (15–25 pF) were obtained from the amplifier "whole-cell capacitance" knob values after total compensation of cell and pipette transients generated by a 10-ms voltage step. Leak currents were subtracted online with a P/4 protocol. Calcium currents were recorded in the presence of extracellular TTX (1 μM) and TEA-Cl (10 mM).

EPSCs were evoked by stimulating the globular bushy cell axons in the trapezoid body at the midline of the slice using a bipolar platinum electrode and an isolated stimulator (0.1 ms duration and 4–7 V amplitude). Strychnine (1 μM) was added to the external solution to block glycinergic synaptic responses. Presynaptic action potentials (APs) were measured in the whole-cell configuration under current clamp mode. The current clamp intracellular solution contained 110 mM potassium gluconate, 30 mM KCl, 10 mM Hepes, 10 mM Na_2-phosphocreatine, 0.2 mM EGTA, 2 mM MgATP, 0.5 mM LiGTP, and 1 mM $MgCl_2$. Resting membrane potentials ranged from −68 to −78 mV. Electrode series resistance and electrode capacitance were compensated for electronically. APs were elicited using 0.1 to 2 nA/0.25-ms step current pulses. Pregabalin (Gador S.A., Buenos Aires, Argentina) and L-isoleucine were bath-applied.

Data Presentation and Fitting Analysis. Activation curves were obtained from tail currents recorded after depolarizing pulses were repolarized to holding potentials and fitted to a Boltzmann equation:

$$I(V) = I_{max}/(1 + \exp(V_{1/2} - V)/k).$$

The inactivation rate of the presynaptic calcium currents was studied using a paired square-pulses protocol (Patil et al., 1998) and calculated as I_{2PP}/I_{1PP}, corresponding to calcium current inactivation during prepulse [i.e., prepulse (PP) from −75 to −10 mV, applied before an interpulse] or I_{2TP}/I_{1TP} during a test pulse [i.e., test pulse (TP), applied after a depolarizing interpulse from −100 to −10 mV, in 10-mV increments]. The prefix 1 or 2 for both prepulses and test pulses corresponds to the initial or the last 4 ms of the elicited calcium current, respectively (see protocol shown in Fig. 5A).

Activation time constants (τ-on) were obtained by fitting the time course of activation of presynaptic calcium currents evoked by depo-

larizing voltage steps, whereas the time constant of deactivation was measured by fitting the decaying phase of tail currents. Both time courses were fitted by a single exponential function.

PGB dose-response curves were obtained by averaging the percentage of EPSC amplitude reduction at MNTB neurons from different slices. In a few cases, increasing concentrations of PGB were tested in the same neuron. In our hands, the steady-state blocking effect of PGB was observed after 15 min of slice perfusion for all concentrations tested. Dose-response values were fitted to a Hill equation, $I(C) = I_{max}/(1+ C_{50}/C)/n_H)$, using SigmaPlot 10.

Statistical differences were evaluated using SigmaPlot 10 and Statistica 7. Average data are expressed and plotted as means ± S.E.M. Statistical significance was determined using either a repeated-measures ANOVA or Student's t test. The ANOVA comparison was considered significant when $p < 0.05$ and the Student-Newman-Keuls post hoc test when $t < 0.05$.

Drugs and Reagents. All substances used for the preparation of aCSF and recording solutions were purchased from either Sigma-Aldrich (St. Louis, MO) or Merck (Darmstadt, Germany).

Results

Acute Effects of PGB on Evoked EPSCs. A broad range of concentrations of PGB have been used in previous reports (McClelland et al., 2004; Beydoun et al., 2005; Micheva et al., 2006). After a single in vivo administration of PGB, its relevant clinical concentration in plasma was found to reach up to 120 μM (Johannessen et al., 2003), whereas higher concentrations such as 500 μM were expected after multiple doses (plasma half-life ~6 h) (Beydoun et al., 2005). To determine the maximal PGB concentrations with a clear synaptic effect in vitro, we first studied the dose-response curve of PGB on EPSCs recorded from the principal neurons of MNTB (Fig. 1A). We recorded EPSCs (amplitudes of which were independent of stimulus intensity above threshold) during acute slice bathing with aCSF solutions containing 10 μM, 100 μM, 500 μM, and 1 mM PGB. Although 100 μM PGB did not produce a significant effect on synaptic responses in vitro (Fig. 1A, repeated measures ANOVA, $p > 0.05$), EPSCs were significantly reduced by both 500 μM and 1 mM PGB (Fig. 1A, repeated measures ANOVA $F_{2,16} = 10.60$, $p < 0.003$, Student-Newman-Keuls post hoc test, $t < 0.05$). Indeed, mean EPSCs amplitudes were reduced by 30 ± 3% in the presence of 500 μM PGB (Fig. 1, A and B, 10.1 ± 0.6 nA, $n = 12$, and 7.1 ± 0.2 nA, $n = 7$, for controls and after 15 min of 500 μM PGB, respectively; Student's t test, $p = 0.024$). No significant changes on EPSCs amplitudes were observed during 20 min of perfusion with aCSF solution (i.e., under vehicle perfusion conditions). The reduction in EPSC amplitudes was partially rescued (~10%) by L-isoleucine (1.5 mM) (Fig. 1, C, open circles, and D, light gray line and bar). L-Isoleucine is a pharmacological tool used extensively to reverse PGB effects due to its known high affinity for the PGB binding site at α_2-δ subunits (Stewart et al., 1993; Su et al., 2005).

Amplitudes of miniature EPSCs (mEPSCs) in the presence of TTX (1 μM) can be considered good estimates of quantal size (Fig. 2). We found that the frequency of spontaneous events was drastically reduced in the presence of PGB (Fig. 2B, 0.5 ± 0.1 Hz, + 500 μM PGB compared with 1.7 ± 0.4 Hz, −PGB condition; Student's t test, $p = 0.004$), whereas no differences were found in their mean amplitudes (Fig. 2C, 39 ± 2 pA in −PGB, $n = 11$ and 38 ± 2 pA in +PGB, $n = 10$). These results suggest a presynaptic acute action of PGB, reducing spontaneous neurotransmitter release at the calyx of Held-MNTB synapses.

Acute Modulation of I_{pCa} by Pregabalin. On the basis of the PGB dose-response presented above, we decided to investigate the effect of PGB (500 μM) on I_{pCa}. We evoked I_{pCa} with 50-ms depolarizing voltage ramps using normal aCSF solution (Fig. 3A, inset, voltage range −75 mV to +60 mV). This protocol allowed us to study the effects of PGB on both amplitude- and voltage-dependent activation of calcium currents while mini-

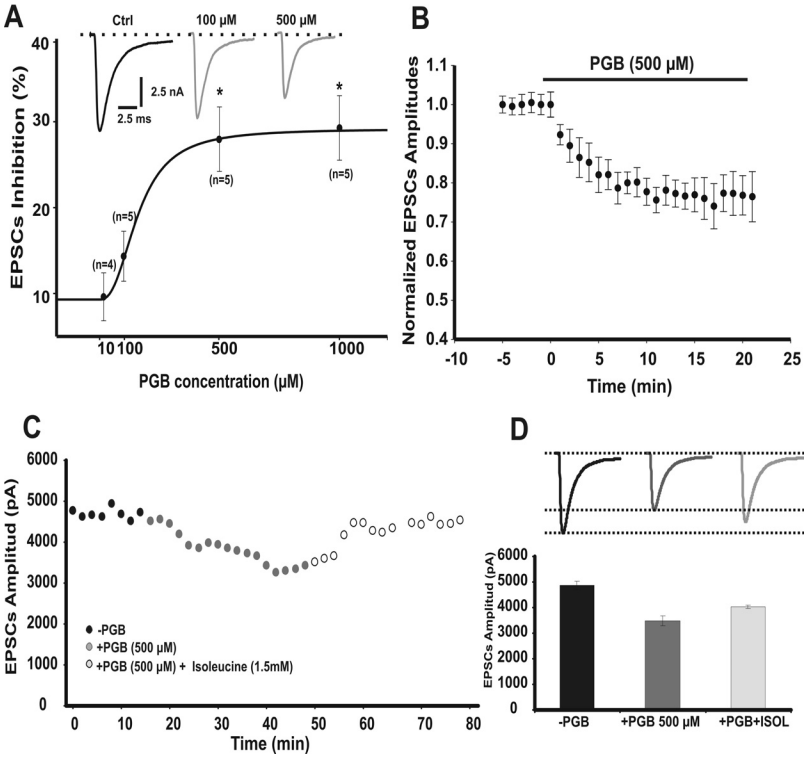

Fig. 1. PGB reduces excitatory postsynaptic currents. A, dose-response relationship fitted to a Hill equation (IC_{50} = 161.13 μM, Hill slope 2.4663). EPSC amplitudes after the inhibitory effect of PGB at both 500 μM and 1 mM concentrations were statistically different with respect to control conditions (repeated measures ANOVA $F_{2,16} = 10.60$, $p < 0.003$, Student-Newman-Keuls post hoc test, $t < 0.05$). Top inset, representative traces of EPSCs in control (Ctrl) conditions and after a 15-min incubation with two different PGB concentrations. B, time plot of EPSC normalized amplitudes from MNTB neurons (−75 mV holding potential) before and during bath perfusion with 500 μM PGB (top black solid bar). Mean EPSC amplitude was reduced by 30 ± 3% (Student's t test, $p = 0.024$). Note how the EPSC maximum inhibition reached a steady-state value after 10 min of PGB bath application. C, EPSC amplitudes in the absence (black circles) or in the presence of PGB (500 μM, gray circles) and after L-isoleucine application (1.5 mM, open gray circles). D, the PGB effect was partially rescued (up to 10%) by L-isoleucine. Values are presented as means ± S.E.M.

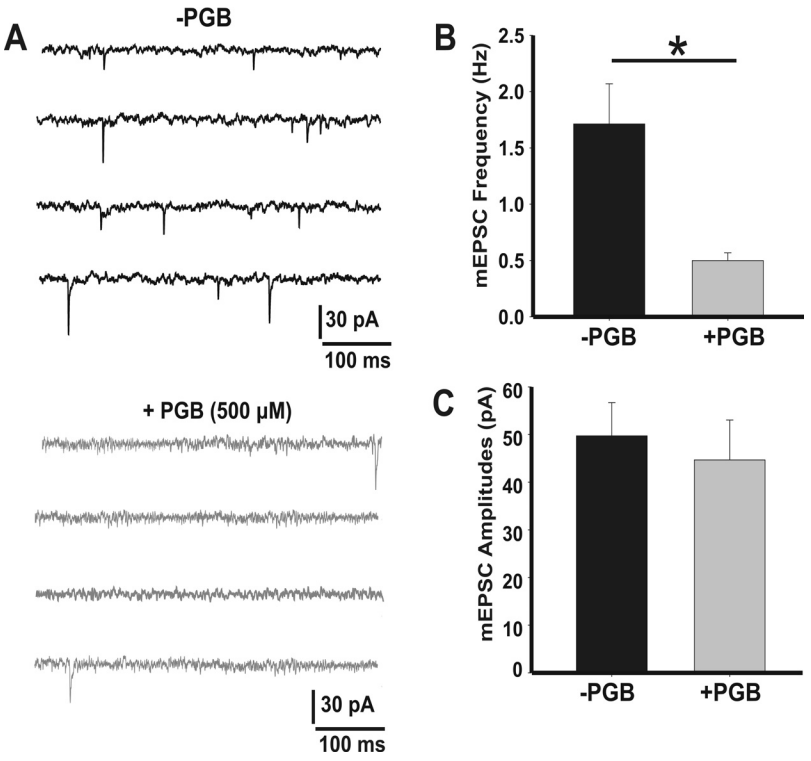

Fig. 2. Frequencies, but not amplitudes, of spontaneous EPSCs are reduced by PGB. A, representative traces of mEPSPs (in the presence of 1 μM TTX) in the absence (top) or presence (bottom) of 500 μM PGB. B and C, mean mEPSC frequencies and amplitudes, respectively. mEPSPs were recorded during 3 min. Mean amplitudes were 39 ± 2 pA in −PGB (n = 11) and 38 ± 2 pA in +PGB (n = 10), whereas frequencies were 1.7 ± 0.4 and 0.5 ± 0.1 Hz, respectively (∗, Student's t test, p = 0.004). Values are presented as mean ± S.E.M.

mizing its rundown. At the age period used in this work (postnatal days 11 to 15), only P/Q type calcium channels mediate neurotransmitter release at the presynaptic calyx of Held (Iwasaki and Takahashi, 1998; Inchauspe et al., 2004; Fedchyshyn and Wang, 2005). Peak I_{pCa} amplitudes observed after a 15-min bath application of PGB were reduced by 30% (Fig. 3A, filled gray circles) and were partially rescued up to 10% by 1.5 mM L-isoleucine (1.5 mM, Fig. 3A, empty gray circles). In addition, L-isoleucine itself did not affect calcium currents (Supplemental Fig. 1, A and B). Therefore, acute PGB was able to reduce calcium currents by a mechanism involving interactions with PGB and the L-isoleucine receptor, the α_2-δ auxiliary subunits of the calcium channel.

Furthermore, we examined the effects of PGB on the current-voltage (I-V) relationship of I_{pCa}. We observed that calcium current density values (peak values at −15 mV) were significantly reduced by 500 μM PGB (Fig. 3B, left, representative current traces on the right). Mean calcium current densities were −28.3 ± 3.9 pA/pF for −PGB and −16.5 ± 5.0 pA/pF for +PGB conditions (repeated measures ANOVA, $F_{2,\,214}$ = 19.594, $p < 0.001$, Student-Newman-Keuls post hoc test, $t < 0.01$). Steady-state activation curves, obtained by plotting tail current peak amplitudes versus step pulse voltage (Fig. 3C), were not significantly different when −PGB and +PGB conditions were compared. Half-activation ($V_{1/2}$) voltages were −28.9 ± 0.4 mV (n = 11) in −PGB and −28.3 ± 0.5 mV (n = 11) in +PGB conditions, and slope factors were also similar: k = 5.7 ± 0.4 mV (−PGB) and 5.4 ± 0.4 mV (+PGB) (Student's t test, $p > 0.05$, n = 11).

We analyzed the voltage dependence of I_{pCa} time constants of activation (τ-on) and deactivation (τ-off) obtained from the initial part of square depolarizing pulses or their repolarizing phase of tail currents, respectively (Fig. 4). Both activation and deactivation kinetics were faster in the presence of 500 μM PGB, thus suggesting a dual PGB effect by reducing I_{pCa} amplitudes while accelerating calcium channel kinetics of opening and closing.

I_{pCa} Inactivation Properties Are Targeted by PGB. Acute PGB was initially observed to remove current inactivation during depolarizing square pulses (Fig. 3B, right, +PGB). We continued characterizing acute PGB effects on inactivation properties of $Ca_v2.1$ calcium channel-mediated I_{pCa} by comparing the rate of inactivation using a three square pulses protocol (Fig. 5A; see Patil et al., 1998). A first prepulse generated calcium currents that inactivated along the pulse. Thus, the calcium current ratio measured at the beginning and at the end of the prepulse (I1 and I2 PP, respectively) gave us information about the calcium channel inactivation during prepulse (Fig. 5B). Similar to prepulse, calcium currents at the beginning and at the end of the test pulse (I1 and I2 TP, respectively) were compared. A second pulse or interpulse (IP) was used to modulate deactivation/inactivation of calcium channels before the TP. We measured calcium currents at the end of interpulse (Fig. 5C).

In control conditions, there was a 10% prepulse inactivation rate (I_{2PP}/I_{1PP}), which was drastically reduced in the presence of PGB (Fig. 5B, 0.90 ± 0.03 for −PGB, n = 16 and 0.99 ± 0.01 for +PGB, n = 6, Student's t test, p = 0.042). Such an effect was further characterized by analyzing the test pulse inactivation rate (I_{2TP}/I_{1TP}). Although clear inactivation was detected in the absence of PGB, in the presence of a 500 μM concentration of the drug a larger difference in current inactivation was observed (Fig. 5D, □ plot versus ▲ plot). Significant differences in the voltage-dependent I_{2TP}/I_{1TP} ratio were observed (slopes: −PGB = $9 \pm 3 \times 10^{-4}$ mV^{-1} and +PGB = $2 \pm 1 \times 10^{-4}$ mV^{-1}, Student's t test, p = 0.025). Furthermore, 100 μM PGB (a plasma concentration within clinical range) was also capable of rescuing I_{pCa} from inactivation (Fig. 5D, open triangles, slope: $-6 \pm 3 \times 10^{-4}$ mV^{-1}, Student's t test, p = 0.001). The inactivation previously ob-

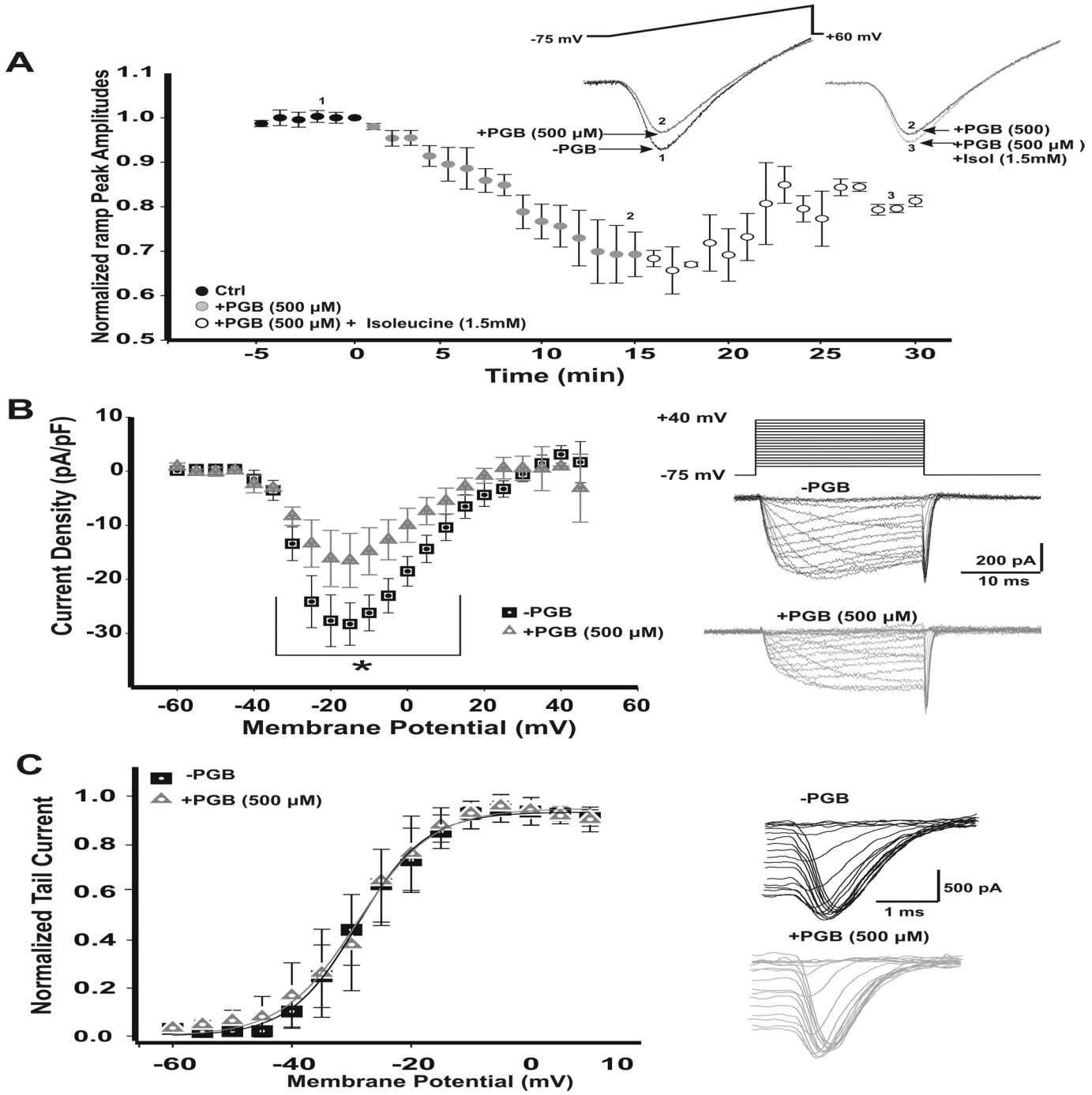

Fig. 3. Acute reduction of presynaptic calcium currents (I_{pCa}) by PGB. A, peak current amplitudes observed for 50-ms depolarizing voltage ramps either after bath perfusion with 500 µM PGB (filled gray circles, $n = 7$) or with the combination of PGB + 1.5 mM isoleucine (Isol; open gray circles, $n = 3$). PGB reduced calcium currents (I_{pCa}) by 30%, whereas in the presence of PGB + isoleucine, I_{pCa} recovered 10% above control amplitudes. Stimulus ramp protocols with their representative I_{pCa} are shown in the right inset. Numbers from 1 to 3 indicate the specific time points of the representative traces illustrated. B, current density-voltage relationships for I_{pCa} before (−PGB) and after a 15-min bath perfusion with PGB (+PGB). The I_{pCa} started activating at −35 mV with an apparent reversal potential at +40 mV. Peak inward current density was reached at −15 mV with mean values of −28.3 ± 3.9 pA/pF for −PGB and −16.5 ± 5.0 pA/pF for +PGB (*, repeated measures ANOVA, $F_{2,214} = 19.594$, $p < 0.001$, Student-Newman-Keuls post hoc test, $t < 0.01$). Stimulus waveform for the I-V protocol (holding potential −75 mV, voltage square pulses ranging from −60 to +50 mV, 5-mV steps, 20-ms duration) is shown together with representative recordings of I_{pCa} -PGB (top, black) and +PGB (bottom, gray). Current amplitudes are the mean during the last 5 ms of the recordings for each potential. C, I_{pCa} activation curves, obtained from tail currents (see representative tails currents shown in right panels). Activation curves were fitted using a Boltzmann equation. I_{pCa} activated at the same voltages at both conditions. Half-activation voltages ($V_{1/2}$) were 28.9 ± 0.4 mV for −PGB ($n = 11$) and 28.3 ± 0.5 mV for +PGB ($n = 11$, Student's t test, $p > 0.05$). Slopes (k) were 5.7 ± 0.4 and 5.4 ± 0.4 mV (Student's t test, $p > 0.05$) for −PGB and +PGB, respectively. Values are presented as means ± S.E.M.

served in control conditions was abolished when barium replaced calcium as the charge carrier (Supplemental Fig. 2A).

The similarity in mean steady-state current-voltage relationships observed during the interpulse for control (Fig. 5C, −PGB, squares) and +PGB (Fig. 5C, triangles, 100 and 500 µM; repeated measures ANOVA $p > 0.05$) supports the hy-

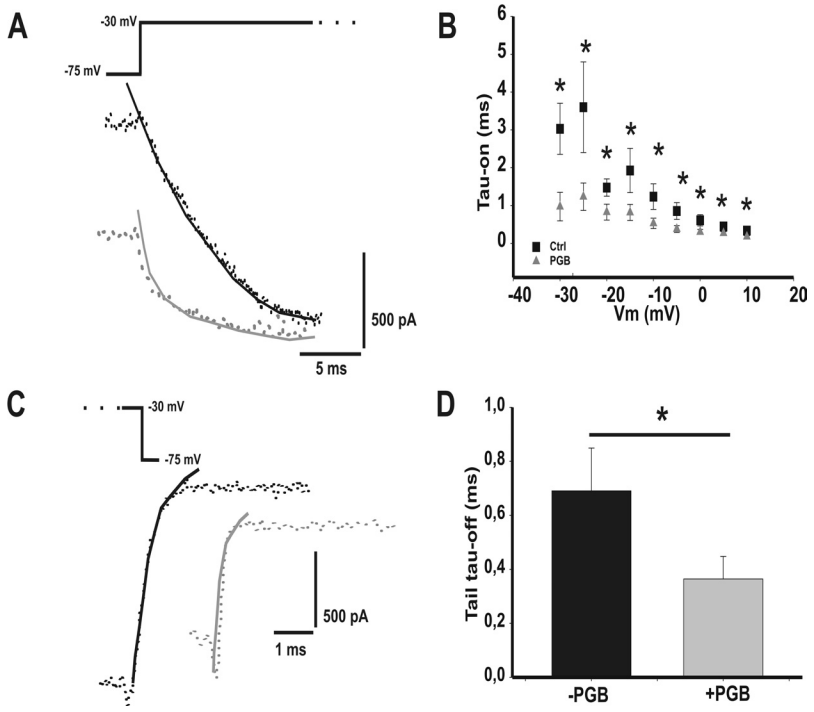

Fig. 4. Effect of PGB (500 μM) on calcium current activation and deactivation time courses. A, representative traces (dotted lines) of I_{pCa} at −30 mV without (black) and with (gray) pregabalin obtained from the I-V protocol. Current traces were fitted (solid line) with a single exponential function. B, I_{pCa} activation time constants (τ-on) plotted against the voltage command step. There are significant differences between −PGB ($n = 10$) and +PGB ($n = 5$; 500 μM) all over the voltage range from −30 mV to +10 mV (∗, Student's t test, $p < 0.05$). C, representative traces (dotted lines) of tail currents after repolarizing to −75 mV from a depolarizing pulse at −10 mV without (black) and with (gray) pregabalin, obtained from the I-V protocol. Currents were fitted (solid line) with a single exponential function. D, deactivation time constant at −10 mV (τ-off) obtained from tail current decaying phase is plotted. Significant differences between −PGB ($n = 12$) and +PGB ($n = 4$) conditions was found (∗, Student's t test, $p < 0.05$, $n = 12$). Values are represent as means ± S.E.M.

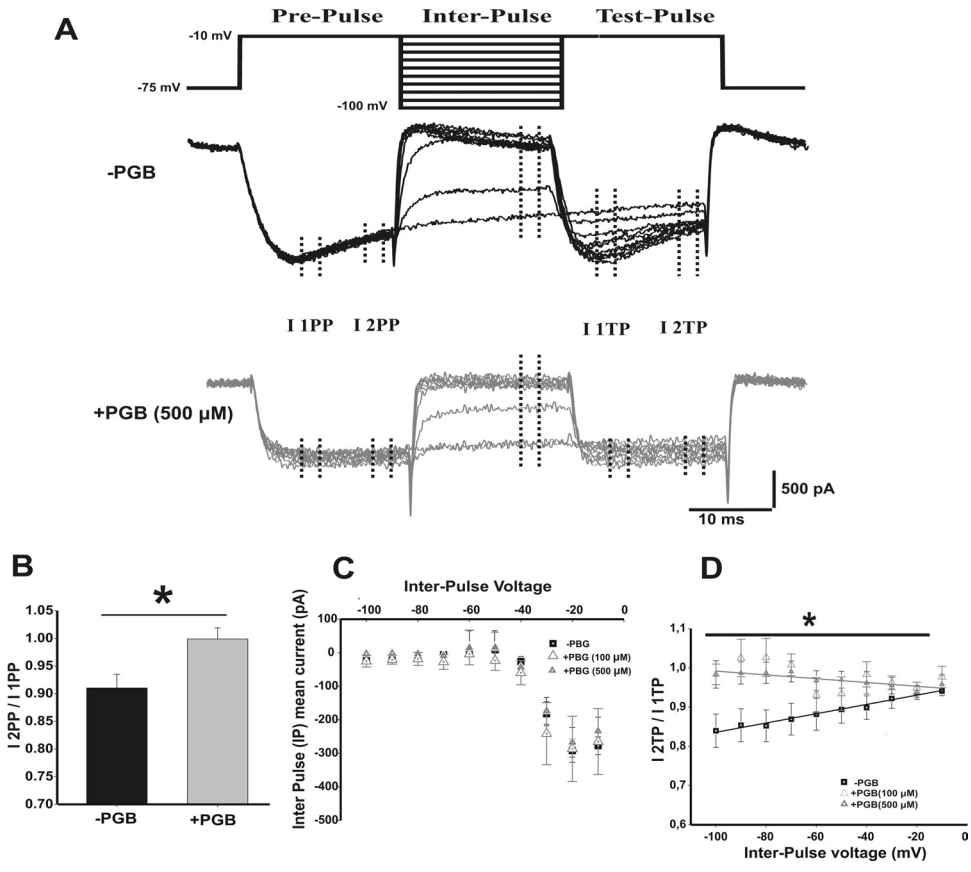

Fig. 5. PGB eliminates the recovery from inactivation of presynaptic calcium currents, without affecting their voltage-dependent activation. A, inactivation protocol (top) consisting of paired square pulses separated by depolarizing voltage steps (interpulse voltage V_{IP} from −75 to −10 mV, 10-mV increments) and representative calcium currents (bottom) are shown for −PGB (black) and +PGB (500 μM) (gray) conditions. Note how steady-state inactivation during both prepulse and test pulses was reduced by PGB. B, inactivation rate during the prepulse (I_{2PP}/I_{1PP}) was 10% in normal conditions and was largely reduced by PGB bath application. C, mean steady-state current versus interpulse voltage relationship for control (−PGB, squares) and 100 μM (+PGB, open triangles) or 500 μM (+PGB, closed triangles). Note the similarity of curves under the three different conditions (repeated measures ANOVA, $p > 0.05$). D, inactivation rate during the test pulse (I_{2TP}/I_{1TP}) versus V_{IP}. The slope of the lineal fitting was $9 \times 10^{-4} \pm 3 \times 10^{-4}$ mV^{-1} for −PGB, $-6 \times 10^{-4} \pm 3 \times 10^{-4}$ mV^{-1} for +PGB (100 μM) (Student's t test, $p = 0.001$), and $2 \times 10^{-4} \pm 1 \times 10^{-4}$ mV^{-1} for +PGB (500 μM) (Student's t test, $p = 0.025$).

pothesis of a dual blocking/recovering of I_{pCa} by acute PGB. Indeed, the loss of calcium channels by the blocking effect of PGB can be promptly compensated for by the rescue of other calcium channels from the inactivation due to PGB.

We continued using a long conditioning prepulse protocol to further characterize the PGB effects on calcium channel steady-state inactivation. We used depolarizing prepulses from −75 to −15 mV (2.5-mV steps) of 2.5-s duration to allow calcium channel inactivation (Fig. 6A), followed by a 50-ms test pulse to quantify the ratio of channels still available to be open. Figure 6A shows representative I_{pCa} from calyx of Held terminals in −PGB (Fig. 6A, upper black traces) and

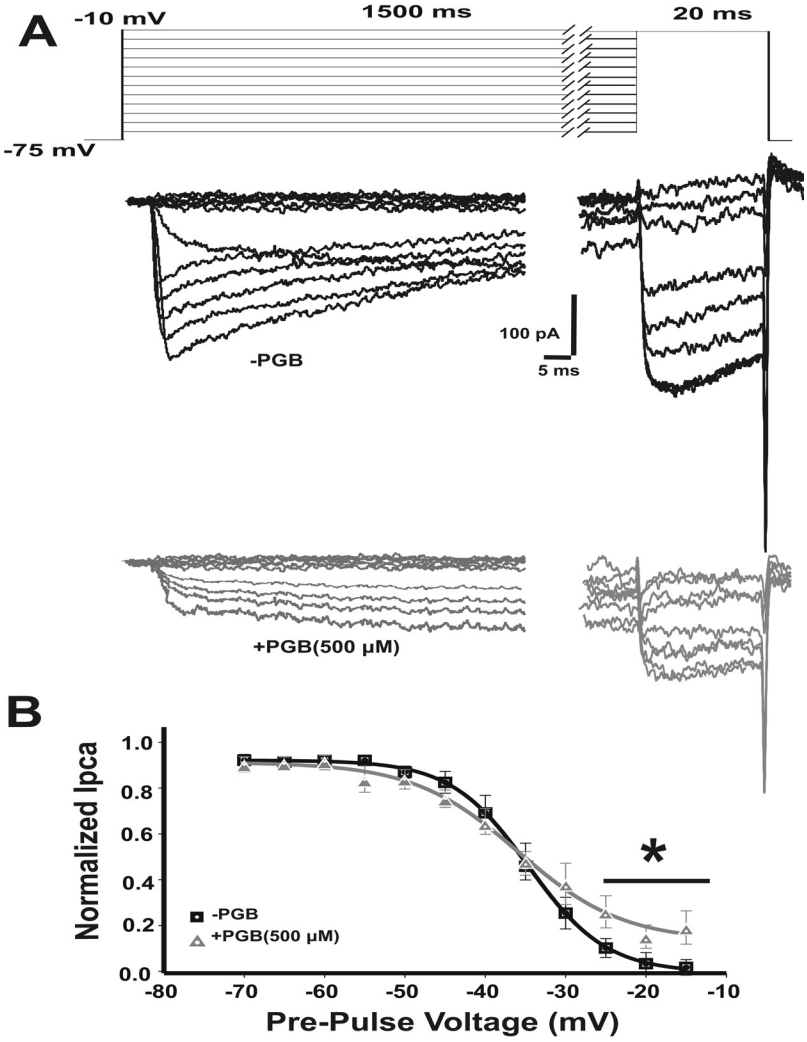

Fig. 6. I_{pCa} steady-state inactivation is modulated by PGB. A, stimulation protocol and sample traces of I_{pCa} with (gray) and without (black) PGB, evoked by a 20-ms voltage step to the potential corresponding to the peak of the I-V curve, after conditioning prepulses of 1.5 s to voltages ranging from −75 to −10 mV (10-mV steps). B, steady-state inactivation from presynaptic terminals with or without PGB. Test I_{pCa} are normalized to the maximum peak amplitude evoked after the −60 mV conditioning pulse, plotted against the conditioning voltage and fitted by a Boltzmann distribution function. Half-activation voltage is $V_{1/2} = -34.1 \pm 0.9$ mV for −PGB ($n = 9$) and -35.9 ± 1.4 mV for +PGB ($n = 6$, Student's t test, $p > 0.05$). The slope factor is significantly lower in the presence of PGB: -4.1 ± 0.2 and -4.8 ± 0.4 mV for −PGB and +PGB, respectively (Student's t test, $p = 0.05$). Values are presented as means ± S.E.M.

500 μM PGB conditions (Fig. 6A, bottom gray traces). I_{pCa} generated by the test voltage step were normalized to the maximum peak amplitude, plotted against the prepulse voltage and fitted by the Boltzmann distribution function (Fig. 6B). Half-inactivation voltages ($V_{1/2}$) were similar for both conditions (-34.1 ± 0.9 mV, $n = 9$ for −PGB and -35.9 ± 1.4 mV, $n = 6$ for +PGB, Student's t test, $p > 0.05$), but slope factors k were significantly reduced in the presence of PGB: -4.8 ± 0.4 mV and -4.1 ± 0.2 mV for −PGB and +PGB, respectively (Student's t test, $p = 0.05$). Moreover, in the presence of PGB, peak currents elicited by prepulse depolarizations greater than −25 mV reached a "plateau" of bigger I_{pCa} amplitudes (Fig. 6B). This result indicates that PGB did not affect half-inactivation voltage but allowed more calcium channels to remain open, in agreement with our previous results.

In conclusion, both low (100 μM) and high (500 μM) PGB concentrations accelerate $Ca_v2.1$ calcium channel recovery from steady-state inactivation, allowing them to be ready to open during successive depolarizations.

Acute PGB Effects on I_{pCa} Elicited by Action Potential Waveforms. To assess the effect of PGB on calcium influx during presynaptic nerve APs, we studied the acute effect of PGB on the calcium currents evoked by AP waveforms previously recorded under current clamp mode (Fig. 7A). We found that the mean calcium density evoked by a single AP was reduced 14 ± 5% in the presence of PGB (31.5 ± 3.4 pA/pF for −PGB and 26.4 ± 2.7 pA/pF for +PGB, paired Student's t test, $p = 0.006$, $n = 14$). In addition, I_{pCa} have been shown to facilitate during repetitive stimulation (Borst and Sakmann, 1998; Cuttle et al., 1998; Inchauspe et al., 2004). We continue studying the effects of acute PGB bath application on I_{pCa} facilitation during either paired pulses or 100-Hz trains of APs (Fig. 7, B and C). I_{pCa} paired pulse facilitation was slightly reduced by 500 μM PGB (mean I_{pCa} facilitation ratios: 1.05 ± 0.01 and 1.03 ± 0.01 for −PGB and +PGB, respectively; Student's t test, $p = 0.03$) (Fig. 7B), whereas a clear reduction on the facilitation rate was observed during 100-Hz train stimulation. Figure 7D shows the time course of calcium current amplitudes versus number of APs, normalized to the amplitude of the first I_{pCa} evoked by the train. In control conditions, a clear I_{pCa} facilitation was observed (112 ± 2%, $n = 15$), which was reduced by PGB (106 ± 4%, $n = 9$; repeated measures ANOVA $F_{2, 284} = 36.99$, $p < 0.001$, Student-Newman-Keuls post hoc test, $t < 0.001$) (Fig. 7D). However, similar I_{pCa} facilitation was obtained at 100 Hz for both Ca^{2+} with PGB- and Ba^{2+}-mediated currents (Supplemental Fig. 2B). Furthermore, the barium current facilitation was similar in the absence (maximum at 104 ± 3%, $n = 3$) or in the presence of 500 μM PGB (106 ± 6%, $n =$

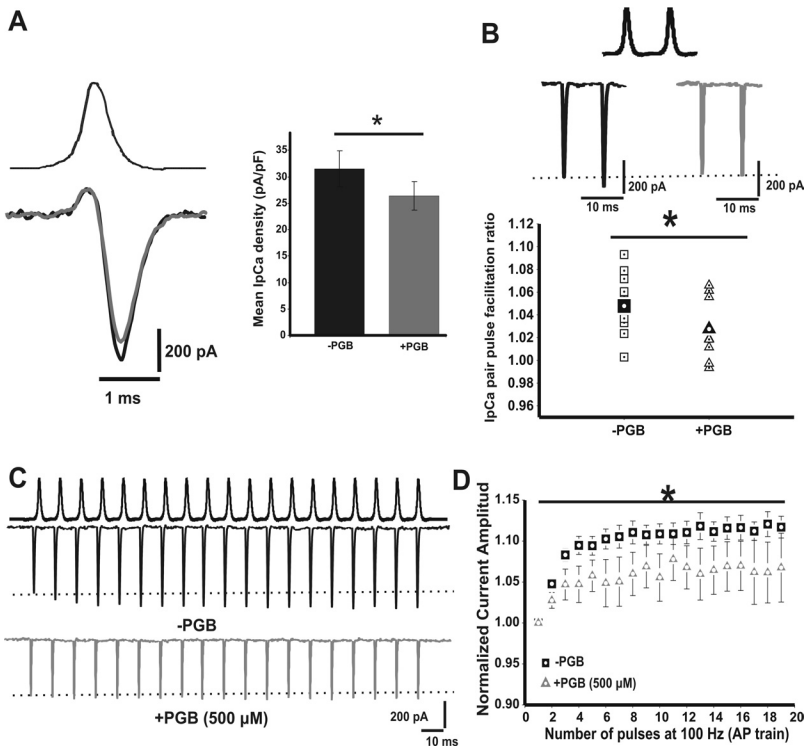

Fig. 7. PGB decreases I_{pCa} facilitation during paired-pulse and high frequency trains of action potentials. A, representative traces of I_{pCa} (left, bottom traces) evoked by a single AP waveform (left, upper trace) recorded at the calyx of Held presynaptic terminals. Mean AP evoked I_{pCa} density (right) is 31.5 ± 3.4 pA/pF for −PGB and 26.4 ± 2.7 pA/pF for +PGB (500 µM). I_{pCa} density decreased 14 ± 5% in the presence of PGB (paired Student's t test, $p = 0.006$, $n = 14$). B, representative paired I_{pCa} traces evoked by paired action potentials (at 100 Hz) recorded in current clamp configuration (top), in both the absence (middle left, black traces), and presence of PGB (500 µM, middle right gray traces). Plot of I_{pCa} ratios (bottom) in −PGB (squares, mean 1.05 ± 0.01) and +PGB (triangles, mean 1.03 ± 0.01, Student's t test, $p = 0.03$). C, representative I_{pCa} traces generated by 100-Hz trains of APs before (top) or after (bottom) PGB bath application. D, normalized current amplitudes during 100 Hz. train of APs. I_{pCa} facilitation observed in the absence of PGB (maximum at 112 ± 2%, $n = 15$) was attenuated in the presence of 500 µM PGB (106 ± 4% after the third shock, $n = 9$; repeated measures ANOVA, $F_{2, 284} = 36.99$, $p < 0.001$, Student-Newman-Keuls post hoc test, $t < 0.001$).

3). These results suggest that PGB-mediated reduction of intrinsic short-term facilitation of $Ca_v2.1$ channels was calcium-dependent.

Discussion

Our results suggest that PGB modulates glutamatergic neurotransmission at the calyx of the Held-MNTB synapse in four ways: 1) reducing presynaptic Ca^{2+} influx through $Ca_v2.1$ channels, 2) decreasing the number of inactivated presynaptic $Ca_v2.1$ channels, 3) decreasing short-term facilitation of presynaptic $Ca_v2.1$ channels, and 4) accelerating the τ-on of calcium channels. There have been few reports showing acute PGB blocking effects on calcium currents at either cultured neurons (Martin et al., 2002; Sutton et al., 2002) or heterologous systems (Hendrich et al., 2008) or PGB-mediated reduction of synaptic transmission at both cultured hippocampal neurons (Micheva et al., 2006) and neuromuscular junction (Joshi and Taylor, 2006). Eroglu et al. (2009) demonstrated that the α_2-δ subunit is involved in excitatory synapse formation and suggested a therapeutic role for gabapentin (a PGB analog) mediated by the blocking of new synapse formation. However, no clear mechanism for PGB has been proposed to explain its cortical antiepileptic effects.

The results presented here provide a novel mechanism of action underlying acute PGB effects on synaptic transmission. First, PGB was shown to block presynaptic $Ca_V2.1$ channel-mediated currents and, therefore, EPSC amplitudes. In agreement with a previous report (Sutton et al., 2002), blocking calcium channels did not shift the voltage value corresponding to the peak of I_{pCa} or the steady-state activation curves. Second, a significant rescue from inactivation was induced by PGB not only at 500 µM (within the clinical plasma concentration range expected after multiple PGB doses) but also at 100 µM (within the clinical range after a single dose). We consider that PGB acts as a neuromodulator instead of a classic channel blocker of calcium for three reasons: 1) the presence of large tail currents observed during stimulation using square pulses (Fig. 3, B and C, right panels) as well as the results obtained from the double-pulse inactivation protocol (Fig. 5A); 2) the large amount of I_{pCa} (Hori and Takahashi, 2009), remaining even in the presence of PGB; and 3) the maintenance by PGB of the steady-state half-inactivation voltage of P/Q calcium channels unchanged (Fig. 6B) but modified their kinetics of activation, inactivation, and deactivation (Figs. 5D and 6B).

A broad range of concentrations (from 0.25 µM to 1 mM) has been used in previous reports (Bayer et al., 2004; McClelland et al., 2004; Micheva et al., 2006; Hendrich et al., 2008). Furthermore, gabapentin (a PGB analog) was previously described to be 4- to 8-fold more concentrated in the brain than in blood plasma (Taylor et al., 1998; Blake et al., 2007). In our hands, dose-response curves for PGB in vitro reached a maximum blocking "plateau" of synaptic responses at 500 µM. Likewise, PGB rescued $Ca_v2.1$ presynaptic channels from their inactivated state. A bath concentration of 500 µM was further used because this concentration showed a maximum synaptic effect without any drug-associated toxicity. Nevertheless, PGB accumulation can be expected after multiple administrations (i.e., 100 and 500 µM) (Johannessen et al., 2003; Beydoun et al., 2005). The discrepancies between the extracellular PGB concentrations used in this work (i.e., using MNTB mice slices) and the ones used in other preparations (hippocampus, trigeminal nucleus, and heterologous systems) might be related to particular interactions of α_2-δ auxiliary subunits with its cellular environment. In this sense, different studies with recombinant calcium channels have failed to show any acute effects of gabapentin on channel function (Taylor, 2009) as expected by the fact that recombinant channels lack many interact-

ing proteins normally found at synapses (e.g., syntaxin and synaptotagmin).

PGB (500 μM) reduced α-amino-3-hydroxy-5-methyl-4-isoxazolepropionic acid-mediated EPSCs amplitudes by 30% during low-frequency stimulation without affecting their time course as previously observed at both culture dorsal root ganglia (Sutton et al., 2002) and neuromuscular junctions (Joshi and Taylor, 2006). On the other hand, no differences were observed on cumulative histograms of rise and decay times of mEPSCs between either condition (data not shown), suggesting a lack of postsynaptic effect of PGB. Thus, given the calcium cooperativity on glutamatergic neurotransmission at the calyx of the Held-MNTB synapse (Fedchyshyn and Wang, 2005), the PGB-mediated reduction of EPSCs amplitudes was consistent with the small decrease in I_{pCa} (~10–14%) (Fig. 7, A and B).

PGB action on calcium currents (i.e., inhibitory effect on calcium current amplitudes versus its ability to reduced channel inactivation) seemed to be related to the population of calcium channels being activated. The total number of activated calcium channels using the square pulses protocol was larger compared with AP waveforms. With use of the former protocol PGB had a predominant effect on the rescue from inactivation of $Ca_v2.1$ presynaptic channels (Fig. 5D), whereas use of the later PGB effects on the inhibition of the calcium current is more relevant (Fig. 7A). Calcium currents elicited by an action potential are "tail current"-like, less affected by PGB than those recorded with long depolarizing pulses. One possible explanation underlying this effect would be related to the observed reduction in calcium current activation time constants after PGB treatment. Moreover, a minor contribution could also result from the reduction in steady-state inactivation observed with PGB. In fact, a 30% reduction in EPSCs amplitude and a 10% reduction in action potential-triggered calcium currents are consistent with a cooperativity of 3 (Schneggenburger and Forsythe, 2006). In addition, both the increase in the activation speed of the I_{pCa} and the decrease in the inactivation observed for the $Ca_v2.1$ channels may justify the decrease in presynaptic short-term facilitation.

We consider PGB an important tool to understand the physiological role of the α_2-δ auxiliary subunit of voltage-gated calcium channels. Several calcium-dependent processes such as calcium current inactivation (Fig. 5A) and facilitation (Fig. 7D) were abolished using barium as the charge carrier (Supplemental Fig. 2). These results shed light on the effects of α_2-δ subunits on the biophysical properties of calcium channels and their physiological function.

Possible Antiepileptic Actions of Pregabalin. Several article have reported a close relationship between alterations on ion channels and different neurologic pathologic changes (channelopathies). In focusing on calcium channels, pathologic conditions such as migraine, ataxia, or epilepsy have been associated with mutations on the α subunit of $Ca_v2.1$, P/Q type calcium channels (Terwindt et al., 1997; Burgess and Noebels, 1999; Pietrobon, 2005). Therefore, migraine and epilepsy may be closely related not only in their etiology (Fletcher et al., 1996; Terwindt et al., 1997; Noebels, 2001) (i.e., genetic), but also in their treatment (Welch, 2005; Masdrakis et al., 2008). Thus, a direct modulation of acute PGB on calcium channel α_2-δ subunits may have an impact on reducing Ca^{2+}-dependent potassium currents and may also have antiepileptic effects. In the hippocampus dentate gyrus, alterations of the existing fine tuning between big conductance (BK) and small conductance (SK) Ca^{2+}-dependent potassium channels may induce hippocampal synchronization, which leads to temporal lobe epilepsy (Brenner et al., 2005). Indeed, an enhancement of BK over SK channels would preclude dentate granule cells from acting as a "low-pass filter" (i.e., ultimately preventing frontal lobe seizures) (Brenner et al., 2005). Because SK channels are more sensitive to intracellular Ca^{2+} than BK, results presented here fit into a possible PGB-mediated antiepileptic action through the reduction of BK activation by blocking calcium channels during action potentials while enhancing SK channel activation by preventing calcium channel inactivation during long periods of time (Fig. 6B). At the same time, the PGB-dependent elimination of $Ca_v2.1$ channels from inactivation would secondarily favor the recruitment of SK channels, reducing neuronal firing rates. All together, PGB modulation of activation/inactivation properties of $Ca_v2.1$ calcium channels is in accordance with previously observed PGB clinical antiepileptic effects (Taylor et al., 2007).

Although our results describe novel acute PGB mechanisms, one can also speculate that PGB chronic actions on cortical areas would control excitation by partially blocking $Ca_v2.1$-mediated excitatory efferent from pyramid cells, while preventing $Ca_v2.1$ channels from being inactivated during interneuron high frequency repetitive action potential discharges. Thus, PGB might prevent epilepsy-mediated unbalances on the cortical excitation/inhibition ratio. Finally, further characterization of PGB actions on both hippocampal and cortical circuits will be central to understand its pharmacologic action to treat pathologic conditions such as epilepsy and migraine.

Acknowledgments

We thank Professor Dr. J. Gerard Borst, Professor Dr. Annette C. Dolphin, and Dr. Joaquin Piriz for helpful discussion and comments on this manuscript. We thank Maria Eugenia Martin for excellent technical assistance. Pregabalin was a generous gift from Gador S.A. [www.gador.com; Darwin 429 (C1414CUI), Buenos Aires, Argentina].

Authorship Contributions

Participated in research design: Di Guilmi, Urbano, and Uchitel.
Conducted experiments: Di Guilmi and Inchauspe.
Performed data analysis: Di Guilmi.
Wrote or contributed to the writing of the manuscript: Di Guilmi, Urbano, Inchauspe, and Uchitel.

References

Bayer K, Ahmadi S, and Zeilhofer HU (2004) Gabapentin may inhibit synaptic transmission in the mouse spinal cord dorsal horn through a preferential block of P/Q-type Ca^{2+} channels. *Neuropharmacology* **46:**743–749.

Belliotti TR, Capiris T, Ekhato IV, Kinsora JJ, Field MJ, Heffner TG, Meltzer LT, Schwarz JB, Taylor CP, Thorpe AJ, et al. (2005) Structure-activity relationships of pregabalin and analogues that target the α_2-δ protein. *J Med Chem* **48:**2294–2307.

Beydoun A, Uthman BM, Kugler AR, Greiner MJ, Knapp LE, Garofalo EA, and Pregabalin 1008–009 Study Group (2005) Safety and efficacy of two pregabalin regimens for add-on treatment of partial epilepsy. *Neurology* **64:**475–480.

Blake MG, Boccia MM, Acosta GB, Höcht C, and Baratti CM (2007) Opposite effects of a single versus repeated doses of gabapentin on retention performance of an inhibitory avoidance response in mice. *Neurobiol Learn Mem* **87:**192–200.

Borst JG and Sakmann B (1998) Facilitation of presynaptic calcium currents in the rat brainstem. *J Physiol* **513 (Pt 1):**149–155.

Brenner R, Chen QH, Vilaythong A, Toney GM, Noebels JL, and Aldrich RW (2005)

BK channel β_4 subunit reduces dentate gyrus excitability and protects against temporal lobe seizures. *Nat Neurosci* **8:**1752–1759.
Burgess DL and Noebels JL (1999) Voltage-dependent calcium channel mutations in neurological disease. *Ann NY Acad Sci* **868:**199–212.
Cunningham MO, Woodhall GL, Thompson SE, Dooley DJ, and Jones RS (2004) Dual effects of gabapentin and pregabalin on glutamate release at rat entorhinal synapses in vitro. *Eur J Neurosci* **20:**1566–1576.
Cuttle MF, Tsujimoto T, Forsythe ID, and Takahashi T (1998) Facilitation of the presynaptic calcium current at an auditory synapse in rat brainstem. *J Physiol* **512 (Pt 3):**723–729.
Eroglu C, Allen NJ, Susman MW, O'Rourke NA, Park CY, Ozkan E, Chakraborty C, Mulinyawe SB, Annis DS, Huberman AD, et al. (2009) Gabapentin receptor α2δ-1 is a neuronal thrombospondin receptor responsible for excitatory CNS synaptogenesis. *Cell* **139:**380–392.
Fedchyshyn MJ and Wang LY (2005) Developmental transformation of the release modality at the calyx of Held synapse. *J Neurosci* **25:**4131–4140.
Fletcher CF, Lutz CM, O'Sullivan TN, Shaughnessy JD Jr, Hawkes R, Frankel WN, Copeland NG, and Jenkins NA (1996) Absence epilepsy in tottering mutant mice is associated with calcium channel defects. *Cell* **87:**607–617.
Gee NS, Brown JP, Dissanayake VU, Offord J, Thurlow R, and Woodruff GN (1996) The novel anticonvulsant drug, gabapentin (Neurontin), binds to the $\alpha_2\delta$ subunit of a calcium channel. *J Biol Chem* **271:**5768–5776.
Hendrich J, Van Minh AT, Heblich F, Nieto-Rostro M, Watschinger K, Striessnig J, Wratten J, Davies A, and Dolphin AC (2008) Pharmacological disruption of calcium channel trafficking by the $\alpha_2\delta$ ligand gabapentin. *Proc Natl Acad Sci USA* **105:**3628–3633.
Hori T and Takahashi T (2009) Mechanisms underlying short-term modulation of transmitter release by presynaptic depolarization. *J Physiol* **587:**2987–3000.
Inchauspe CG, Martini FJ, Forsythe ID, and Uchitel OD (2004) Functional compensation of P/Q by N-type channels blocks short-term plasticity at the calyx of held presynaptic terminal. *J Neurosci* **24:**10379–10383.
Iwasaki S and Takahashi T (1998) Developmental changes in calcium channel types mediating synaptic transmission in rat auditory brainstem. *J Physiol* **509 (Pt 2):**419–423.
Johannessen SI, Battino D, Berry DJ, Bialer M, Krämer G, Tomson T, and Patsalos PN (2003) Therapeutic drug monitoring of the newer antiepileptic drugs. *Ther Drug Monit* **25:**347–363.
Joshi I and Taylor CP (2006) Pregabalin action at a model synapse: binding to presynaptic calcium channel $\alpha_2\delta$ subunit reduces neurotransmission in mice. *Eur J Pharmacol* **553:**82–88.
Klugbauer N, Marais E, and Hofmann F (2003) Calcium channel $\alpha_2\delta$ subunits: differential expression, function, and drug binding. *J Bioenerg Biomembr* **35:**639–647.
Maneuf YP, Gonzalez MI, Sutton KS, Chung FZ, Pinnock RD, and Lee K (2003) Cellular and molecular action of the putative GABA-mimetic, gabapentin. *Cell Mol Life Sci* **60:**742–750.
Martin DJ, McClelland D, Herd MB, Sutton KG, Hall MD, Lee K, Pinnock RD, and Scott RH (2002) Gabapentin-mediated inhibition of voltage-activated Ca^{2+} channel currents in cultured sensory neurones is dependent on culture conditions and channel subunit expression. *Neuropharmacology* **42:**353–366.
Masdrakis VG, Oulis P, Karakatsanis NA, Potagas C, Kouzoupis AV, and Soldatos CR (2008) Remission of migraine attacks in a patient with depression who is taking pregabalin. *Clin Neuropharmacol* **31:**238–240.
McClelland D, Evans RM, Barkworth L, Martin DJ, and Scott RH (2004) A study comparing the actions of gabapentin and pregabalin on the electrophysiological properties of cultured DRG neurones from neonatal rats. *BMC Pharmacol* **4:**14.
Micheva KD, Taylor CP, and Smith SJ (2006) Pregabalin reduces the release of synaptic vesicles from cultured hippocampal neurons. *Mol Pharmacol* **70:**467–476.
Noebels JL (2001) Modeling human epilepsies in mice. *Epilepsia* **42 (Suppl 5):**11–15.
Patil PG, Brody DL, and Yue DT (1998) Preferential closed-state inactivation of neuronal calcium channels. *Neuron* **20:**1027–1038.
Pietrobon D (2005) Function and dysfunction of synaptic calcium channels: insights from mouse models. *Curr Opin Neurobiol* **15:**257–265.
Qin N, Olcese R, Stefani E, and Birnbaumer L (1998) Modulation of human neuronal α_{1E}-type calcium channel by $\alpha_2\delta$-subunit. *Am J Physiol* **274:**C1324–C1331.
Schneggenburger R and Forsythe ID (2006) The calyx of Held. *Cell Tissue Res* **326:**311–337.
Stefani A, Spadoni F, and Bernardi G (1998) Gabapentin inhibits calcium currents in isolated rat brain neurons. *Neuropharmacology* **37:**83–91.
Stewart BH, Kugler AR, Thompson PR, and Bockbrader HN (1993) A saturable transport mechanism in the intestinal absorption of gabapentin is the underlying cause of the lack of proportionality between increasing dose and drug levels in plasma. *Pharm Res* **10:**276–281.
Su TZ, Feng MR, and Weber ML (2005) Mediation of highly concentrative uptake of pregabalin by L-type amino acid transport in Chinese hamster ovary and Caco-2 cells. *J Pharmacol Exp Ther* **313:**1406–1415.
Sutton KG, Martin DJ, Pinnock RD, Lee K, and Scott RH (2002) Gabapentin inhibits high-threshold calcium channel currents in cultured rat dorsal root ganglion neurones. *Br J Pharmacol* **135:**257–265.
Taylor CP, Gee NS, Su TZ, Kocsis JD, Welty DF, Brown JP, Dooley DJ, Boden P, and Singh L (1998) A summary of mechanistic hypotheses of gabapentin pharmacology. *Epilepsy Res* **29:**233–249.
Taylor CP, Angelotti T, and Fauman E (2007) Pharmacology and mechanism of action of pregabalin: the calcium channel $\alpha_2\delta$ (alpha2-delta) subunit as a target for antiepileptic drug discovery. *Epilepsy Res* **73:**137–150.
Taylor CP (2009) Mechanisms of analgesia by gabapentin and pregabalin–calcium channel α_2-δ [$Ca_v\alpha_2$-δ] ligands. *Pain* **142:**13–16.
Taylor CP and Garrido R (2008) Immunostaining of rat brain, spinal cord, sensory neurons and skeletal muscle for calcium channel alpha$_2$-delta ($\alpha_2\delta$) type 1 protein. *Neuroscience* **155:**510–521.
Terwindt GM, Ophoff RA, Lindhout D, Haan J, Halley DJ, Sandkuijl LA, Brouwer OF, Frants RR, and Ferrari MD (1997) Partial cosegregation of familial hemiplegic migraine and a benign familial infantile epileptic syndrome. *Epilepsia* **38:**915–921.
Welch KM (2005) Brain hyperexcitability: the basis for antiepileptic drugs in migraine prevention. *Headache* **45 (Suppl 1):**S25–S32.

Address correspondence to: Dr. Osvaldo D. Uchitel, IFIBYNE, UBA-CONICET, Intendente Güiraldes 2670, Pabellón 2, Piso 2, Ciudad Universitaria, C1428BGA Buenos Aires, Argentina. E-mail: odu@fbmc.fcen.uba.ar

Pregabalin modulation of neurotransmitter release is mediated by change in intrinsic activation/inactivation properties of CaV2.1 calcium channels.

Mariano N. Di Guilmi, Francisco J. Urbano, Carlota Gonzalez Inchauspe and Osvaldo D. Uchitel

Journal of Pharmacology and Experimental Therapeutics

Supplementary Figure 1

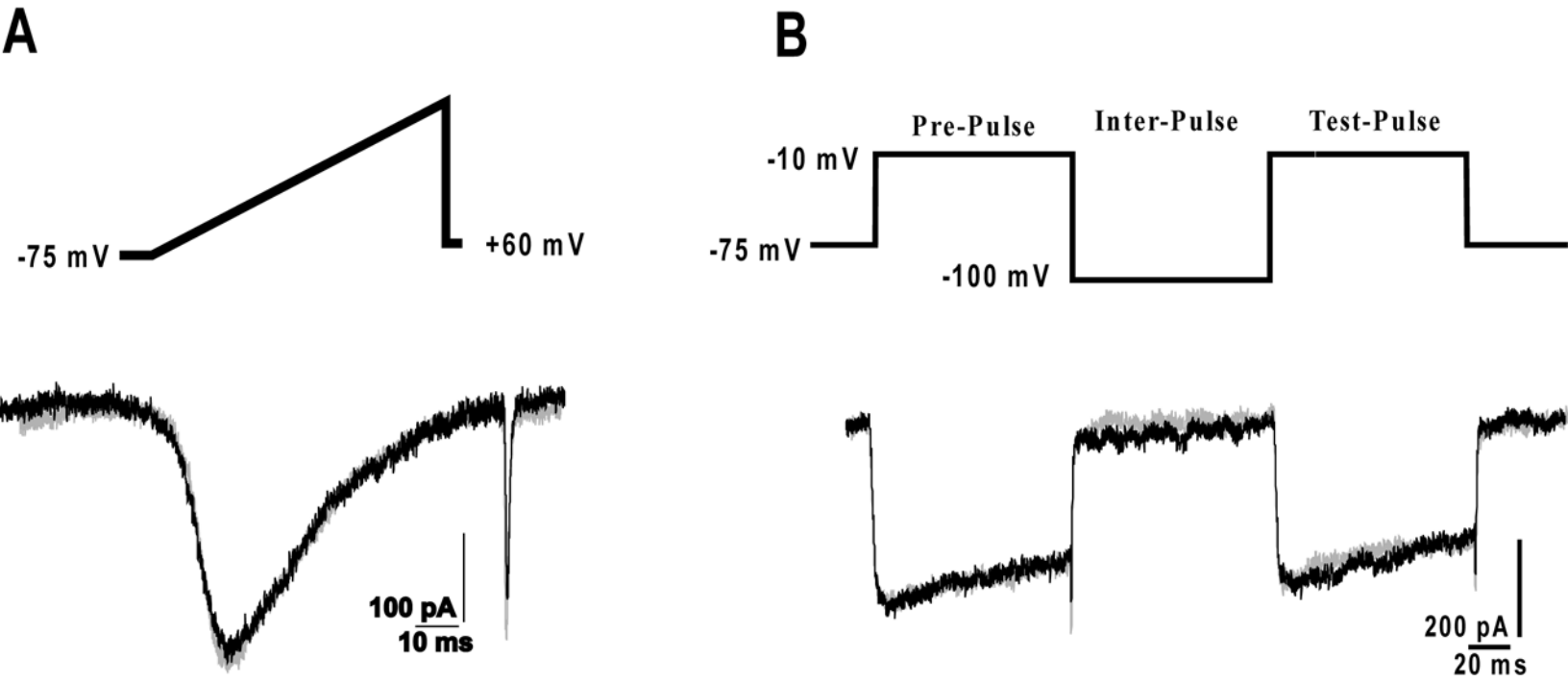

Supplementary Figure 1: Lack of effect of Isoleucine on either IpCa amplitudes or inactivation process.
(A) Peak current amplitudes observed for 50 ms depolarizing voltage ramps either in control condition (black traces) or after bath perfusion with Isoleucine 1.5 mM (grey traces, n = 3). (B) Inactivation protocol (top) consisting of paired square pulses separated by a voltage step at -100 mV and representative calcium currents (bottom) are shown for control (black) and + Isoleucine 1.5 mM (grey).

Pregabalin modulation of neurotransmitter release is mediated by change in intrinsic activation/inactivation properties of CaV2.1 calcium channels.

Mariano N. Di Guilmi, Francisco J. Urbano, Carlota Gonzalez Inchauspe and Osvaldo D. Uchitel

Journal of Pharmacology and Experimental Therapeutics

Supplementary Figure 2

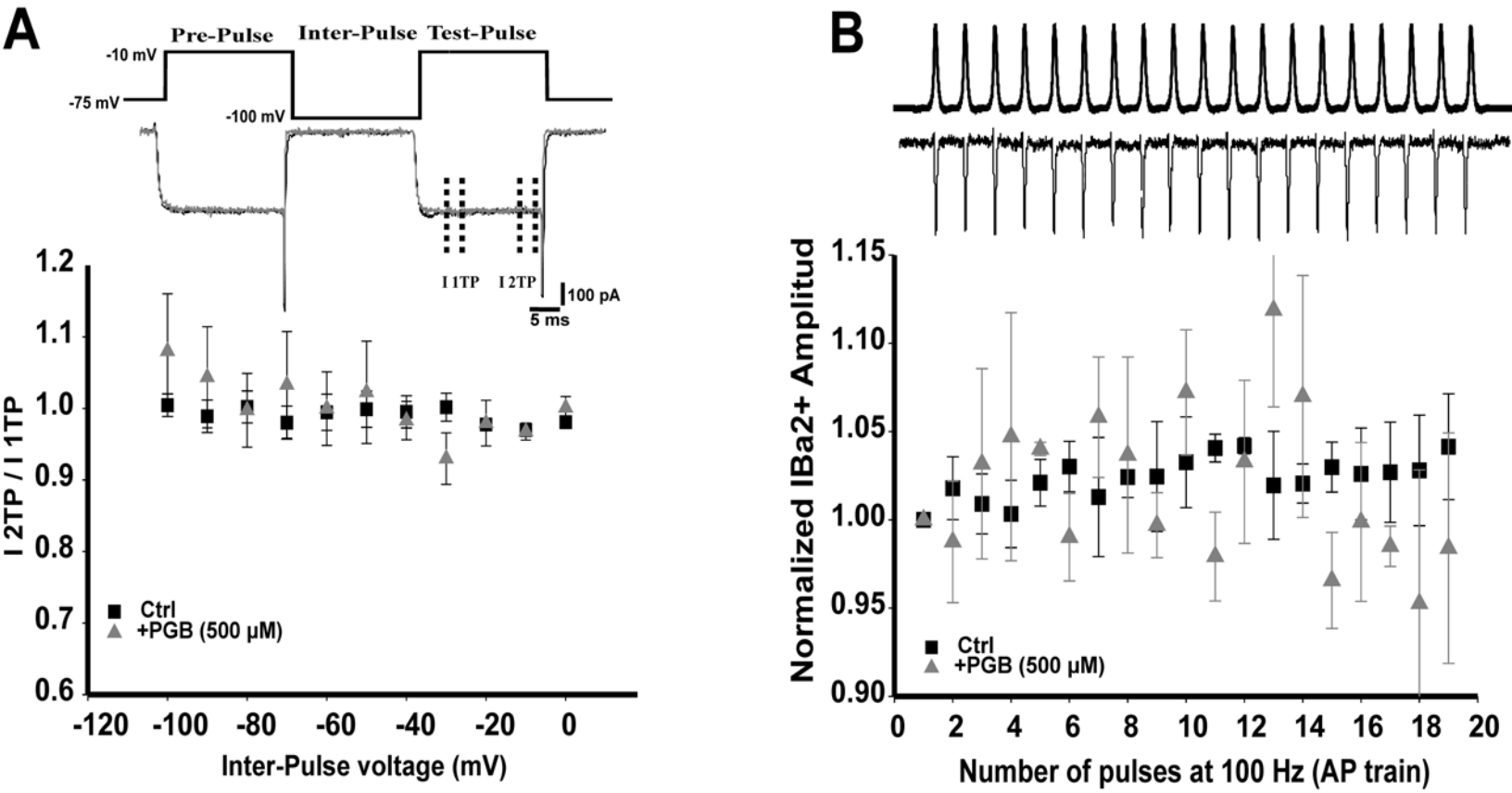

Supplementary Figure 2. Calcium-dependent processes are modified in presence of barium (Ba2+) as the charge carrier.
Ca2+ was replaced by Ba2+ (2 mM) as the charge carrier in the extracellular solution. A. Inactivation protocol consisting of paired square pulses to -15 mV (pre-pulse, PP, and test pulse, TP) separated by depolarizing voltage steps (inter-pulse voltage VIP from -75 mV to -10 mV, 10 mV increments) together with representative calcium currents for an interpulse at -100 mV. are shown for control and +PGB 500 µM condition. I2TP/I1TP ratio at Test-Pulse (TP) versus VIP is plotted (bottom). No significant differences were found between Ctrl and +PGB (500 µM). B. Normalized current amplitudes during 100 Hz. train of APs. Ba++ current facilitation observed in the absence of PGB (maximum of 104±3%, n=3) was similar than in the presence of 500 µM PGB (106±6%, n = 3).